Journal of Engineering Physics and Thermophysics, Vol. 65, No. 3, 1993

APPLYING METHODS OF NUMERICAL MODELING TO OPTIMIZE A PLASMA BURNER OF ATMOSPHERIC PRESSURE

S. M. Perminov, V. N. Perminova, and
A. V. Shakhanov

UDC 532.517

The shape of a plasma burner is optimized by the methods of numerical modeling. Vortex-free flow is created in the burner merely at the expense of selecting the external tube profile rather than by introduction of additional protective flows into the burner.

One of the intensely developing trends in the technology of quartz glass is plasmochemical synthesis of silicon dioxide from high-purity chlorides. In particular, application of plasmochemical methods resulted in creating a new generation of light conductors based on fluorine-doped silica glasses. In a number of methods synthesis is carried out in a plasma burner, the silicon dioxide being removed from the burner by a plasma jet and being directed to the mold with the jet flowing around.

A plasma burner is a section of a quartz tube passing through an HF-inductor or an SHF-waveguide [1, 2]. A twisted gas flow is supplied to the tube via nozzle 1 (Fig. 1a). In such a flow the plasma discharge excited by the electromagnetic field is localized in the near-axis region of the quartz tube and is separated from its walls by an unheated gas layer, which ensures pure conditions of plasmachemical synthesis.

The highest efficiency of transformation of the starting reagents into the final product of synthesis is obtained in supplying the reagents through axial nozzle 2 (Fig. 1b). However, the design shown in Fig. 1b is not viable since recirculation vortices developing between the nozzle cut and the plasma (Fig. 2) return a portion of the silicon dioxide synthesized in the plasma; there occurs blocking of the nozzles, which leads to loss of stability of the plasma flame and degradation of the burner.

One of the variants of designs for plasma burners used in practice is shown in Fig. 1c. By introducing a shielding flow of inert gas via additional annular nozzle 3 one achieves the spacing of the recirculation zone and the zone of synthesis of the product which leads to a decrease in the rate of nozzle overgrowth. A numerical calculation of the characteristics of such a design is given in [3].

For reasons of the complexity of technical realization and maintenance of the design in Fig. 1c one often injects reagents into the flame outside the burner, accepting a considerable decrease in the efficiency of the use of the reagents and energy contributed to the plasma (Fig. 1d).

Using SHF-excitation of the discharge in plasma burners enabled one to realize the technological process of plasmachemical synthesis of fluoride-doped silica glasses for research purposes at lowered capacities and flow rates of the plasma-forming gases [4, 5]. In this connection there arose the problem of miniaturizing plasma burners and simplifying their design without loss in the efficient use of raw materials and energy.

The method of modeling used by the authors made it possible to create vortex-free flow in the burner just by selecting the external tube profile rather than by introducing into the burner additional protective flows. The method used makes it possible to model nonstationary flows in arbitrarily shaped and connected regions (contrary to, for example, [3]) and is therefore applicable to study aerohydrodynamic processes in burners of arbitrary shape, which ensured progress in the problem.

As a mathematical model use is made of a system of hydrodynamic equations that includes nonstationary Navier-Stokes equations written in natural variables and an equation of continuity:

A. A. Blagonravov Institute of Metallography, Russian Academy of Sciences, Moscow. Translated from Inzhenerno-Fizicheskii Zhurnal, Vol. 65, No. 3, pp. 325-331, September, 1993. Original article submitted October 19, 1992.

 1062-0125/93/6503-0890$12.50

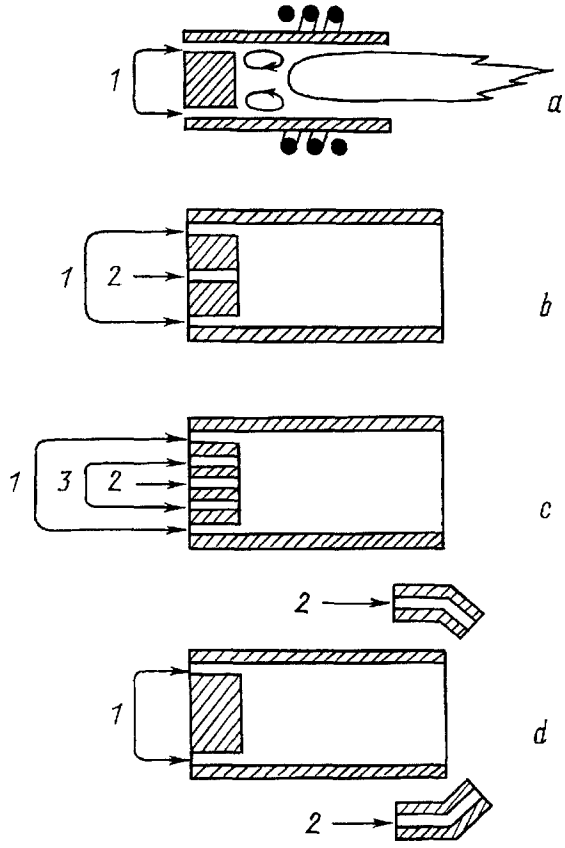

Fig. 1. Designs of plasma burners: a) scheme of the simplest plasma burner; b-d) different variants of reagent supply to the plasma.

$$\frac{\partial \bar{U}}{\partial t} + (\bar{U}\nabla)\bar{U} = -\nabla P + \frac{1}{\mathrm{Re}}\Delta\bar{U}, \quad \mathrm{div}\,\bar{U} = 0. \tag{1}$$

Here t is the time, $U = (U_1, U_2, U_3)$ is the velocity, P is the pressure, $\mathrm{Re} = (U_0 L_0)/\nu$ is the Reynolds number, L_0, U_0 are the characteristic scale of the burner and the characteristic velocity of the flows, ν is the kinematic viscosity. Equations (1) are written in dimensionless form. The possibility of using the assumption of incompressibility follows fromthe fact that the flow velocities in the burner do not exceed 1/3 of the speed of sound. At these velocities variations in the density and temperature of the gas, occurring in the flow field, are relatively small and therefore the gas may be considered incompressible. Such an approach is correct outside the zone of plasma formation, where the investigations have been performed.

The intricacy of the geometric shape leads to the need to use a curvilinear coordinate system in constructing difference schemes. To construct computational grids, the Thompson method was used [5]. This method permits the construction of two- and three-dimensional computational grids of arbitrary connectivity with crowding of the nodes at assumed sites of large gradients of the solution.

In constructing an adapted computational grid we prescribe the mapping of the computational region D in the variables (y_1, y_2, y_3) into the initial region Ω in the variables (x_1, x_2, x_3) [6]. In the region D the image of the initial grid is a uniform orthogonal grid on which the numerical solution of the problem (1) is performed. The differential operators in system (1) in a curvilinear coordinate system have the form

$$\nabla P = \sum_{k=1}^{3}\sum_{j=1}^{3}\frac{\partial P}{\partial y_j}\,y_{jk}\bar{e}_k, \quad \mathrm{div}\,\bar{U} = \frac{1}{J}\sum_{k=1}^{3}\sum_{j=1}^{3}\frac{\partial}{\partial y_j}(y_{jk}JU_k),$$

$$\Delta U_m = \frac{1}{J}\sum_{k=1}^{3}\sum_{i=1}^{3}\sum_{j=1}^{3}\frac{\partial}{\partial y_j}\left(y_{jk}y_{ik}J\,\frac{\partial U_m}{\partial y_i}\right), \quad m = 1, 2, 3,$$

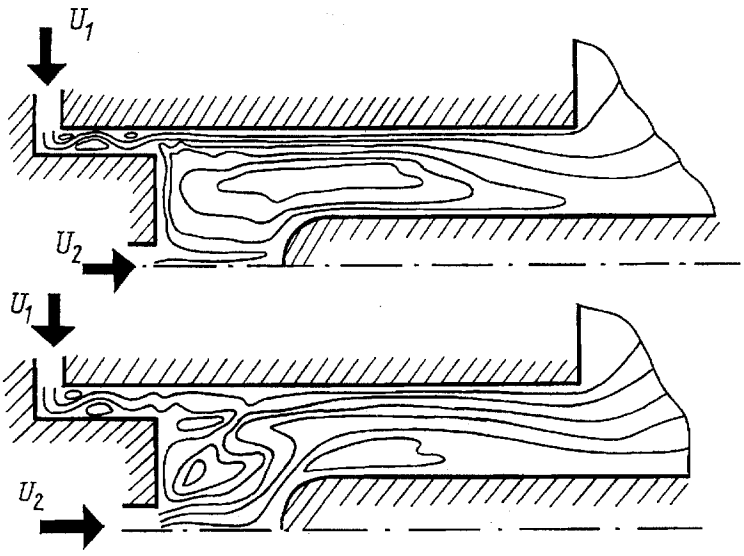

Fig. 2. Vortex formation processes in a plasma burner.

where $\bar{e}_m$ is the unit vector of the x_m axis; $\overline{U} = U_m\bar{e}_m$; J is the Jacobian of the transformation $(x_1, x_2, x_3) \to (y_1, y_2, y_3)$; y_{jk} are the elements of the Jacobi matrix $D(y)/D(x)$, considered as functions of the variables y_1, y_2, and y_3.

When performing the calculations use was made of two different methods for solution of the system of hydrodynamic equations: the method of splitting into physical variables and that of parabolic ε-regularization of the continuity equation. Results of calculations by both methods turned out closely similar.

We define in the region D in question the computational grid: $D_h = \{(y_1, y_2, y_3); y_1 = (i - 1)h_1, y_2 = (j - 1)h_2, y_3 = (k - 1)h_3, i = 1, \ldots, n_1, j = 1, \ldots, n_2, k = 1, \ldots, n_3, (y_1, y_2, y_3) \in \overline{D}\}$ and the grid functions $\overline{U} = \overline{U}(y_1, y_2, y_3)$, $P = P(y_1, y_2, y_3)$. The functions $\overline{U}$ are considered as vectors in the initial coordinate system and are determined at the nodes of the computational grid, and the pressure P - at the centers of cells of the grid D_h. Upon substituting difference operators for the differential ones used, the resulting difference analog of the Navier-Stokes equation is written at the grid nodes, and of the continuity equation - at the centers of the cells. Denoting the difference approximations of the operators div, grad, Δ by div^h, grad^h, Δ^h, we chose them so that the values of $\mathrm{div}^h \overline{U}$, $\mathrm{div}^h\nabla^h P$ occur at the centers of the cells and the values of $\mathrm{grad}^h P$, $\Delta^h\overline{U}$ - at the grid nodes:

$$\mathrm{div}^h\overline{U} = \frac{1}{J}\left(\frac{r_1 + r_1^{+g_2} + r_1^{+g_3} + r_1^{+g_2+g_3}}{4}\right)_{y_1} +$$
$$+ \frac{1}{J}\left(\frac{r_2 + r_2^{+g_1} + r_2^{+g_3} + r_2^{+g_1+g_3}}{4}\right)_{y_2} +$$
$$+ \frac{1}{J}\left(\frac{r_3 + r_3^{+g_1} + r_3^{+g_2} + r_3^{+g_1+g_2}}{4}\right)_{y_3},$$
$$\mathrm{grad}^h P = \left[y_{1m}\left(\frac{P + P^{-g_2} + P^{-g_3} + P^{-g_2-g_3}}{4}\right)_{y_1} +\right.$$
$$+ y_{2m}\left(\frac{P + P^{-g_1} + P^{-g_3} + P^{-g_1-g_3}}{4}\right)_{y_2} +$$
$$\left. + y_{3m}\left(\frac{P + P^{-g_1} + P^{-g_2} + P^{-g_1-g_2}}{4}\right)_{y_3}\right]\bar{e}_P.$$

Here $r_i = J(y_{i1}U_1 + y_{i2}U_2 + y_{i3}U_3)$, $\overline{U}^{+g1} = \overline{U}(\overline{y} + \overline{g}_i)$, i = 1, 2, 3. The single vector $\overline{e}_m$ is the unit vector of the x_m axis of the initial coordinate system, $\overline{g}_i$ is the unit vector of the y_i axis. The operator $\Delta^h f$ appears thus:

$$\Delta f = \frac{1}{J}[(g_{11}f_{y_1})_{\overline{y}_1} + (g_{22}f_{y_2})_{\overline{y}_2} + (g_{33}f_{y_3})_{\overline{y}_3} + (g_{12}f_{\circ y_1})_{\circ y_2} +$$

$$+ (g_{12}f_{\circ y_2})_{\circ y_1} + (g_{13}f_{\circ y_1})_{\circ y_3} + (g_{13}f_{\circ y_3})_{\circ y_1} + (g_{23}f_{\circ y_2})_{\circ y_3} + (g_{23}f_{\circ y_3})_{\circ y_2}],$$

$$g_{ik} = \sum_{m=1}^{3} J y_{lm} y_{mk}.$$

The approximation of the differential operators was constructed in such a way that in the grid analog of the scalar product $L_2(\Omega)$ on the subspace of functions equal to zero on the boundary of the grid region $\overline{D}_h$ the following properties of the difference operators are fulfilled:

a) $\mathrm{div}^h = -(\mathrm{grad}^h)^*$,

b) $-\Delta^h = (-\Delta^h)^* \geq cE$,

c) $-(\mathrm{div}^h \mathrm{grad})^h = [-(\mathrm{div}^h \mathrm{grad})^h]^* \geq cE$.

A scheme with damping [7] was used as an approximation of the convective term $N(\overline{U}, \overline{U})$.

The calculation equations in the splitting scheme appear as follows [8]: let the values of $t_n \in [0, T]$ where [0, T] is the time interval in question, be prescribed. By $\overline{f}^n$ we will denote the value of the function on the n-th time step. Then, to find U^{n+1}, P^{n+1}, use is made of the three-stage scheme

$$\frac{\hat{U} - U^n}{\tau} = \frac{1}{\mathrm{Re}} \Delta^h U^n - (U^n \nabla^h) U^n,$$

$$\Delta^h (P^{n+1}) = \frac{\mathrm{div}^h \hat{U}}{\tau}, \quad \frac{U^{n+1} - \hat{U}}{\tau} = -\nabla^h (P^{n+1}). \tag{2}$$

In the first stage transfer occurs merely by convection and viscosity forces. The obtained intermediate velocity field $\hat{U}$, i.e., the predictor, is corrected in the third stage due to the pressure gradient. In formulating the boundary conditions for pressure the well-known method of elimination was used [8]. We point out that when solving Eqs. (2) the solution to the difference analog of the Poisson equation presents the central problem. The efficiency of applied programs used by the authors is reached due to the application of Kholesskii's method of expansion (LDU-expansion) [10] and the method of conjugate gradients. This work makes use of Kholesskii's expansion in the two-dimensional statement. The method of conjugate gradients ICCG was applied in the three-dimensional statement to solve the Poisson equation with the prior use of the ILU-expansion method [10].

In the parabolic ε-regularization method [11] the basic calculation equations in difference form have the form

$$B\overline{U}_t + (U^n \nabla^h) U^n - \frac{1}{\mathrm{Re}} \Delta^h U^{n+1} + \nabla^h P^{n+1} = 0, \quad \beta\tau A P_t + \mathrm{div}^h U^{n+1} = 0,$$

where $B = B^* > 0$, $A = A^* > 0$ are the iteration operators; $B \simeq E$, β is the iteration parameter; $\beta\tau = \varepsilon \ll 1$, $\overline{U}_t = (\overline{U}^{n+1} - \overline{U}^n)/\tau$, $P_t = (P^{n+1} - P^n)/\tau$. The system of equations (3) prescribes a whole series of schemes. The specific form of the scheme is determined by the choice of the operators B and A. We used the operators

$$B = E + \frac{\tau^2}{\mathrm{Re}^2} R_1 R_2 + \frac{\tau}{\beta} \nabla^h A^{-1} \mathrm{div}^h,$$

$$A = (E + \omega A_1)(E + \omega A_2), \quad -\Delta^h = R_1 + R_2, \quad -\mathrm{div}^h \mathrm{grad}^h = A_1 + A_2,$$

where $R_1 = R_2^* > 0$, $A_1 = A_2^* > 0$, R_1, R_2, A_1, and A_2 are the triangular matrices.

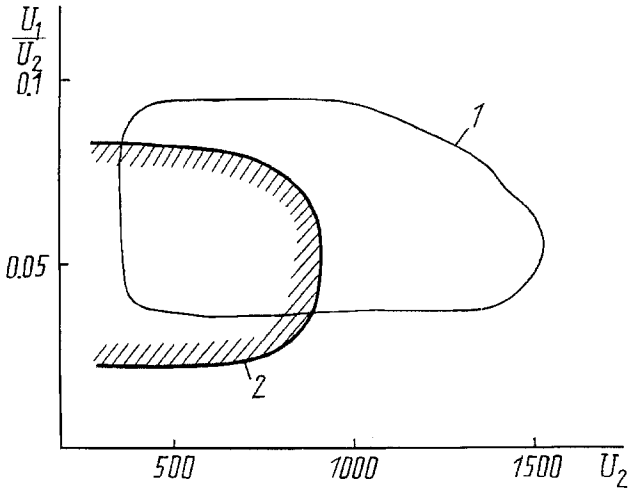

Fig. 3. Zone of vortex-free flow in a plasma burner of the simplest design: U_1, U_2 are the velocities of gas flows respectively through the annular and central nozzle (cm/sec), 1) numerical experiment, 2) natural experiment.

The parameter ω, as the practice of calculations of different problems has shown, is optimally determined only from the characteristics of the spatial grid. With such a choice of the operators B and A the system of equations (3) can be rewritten in the following form:

$$\left(E + \frac{\tau}{\mathrm{Re}} R_1\right)\left(E + \frac{\tau}{\mathrm{Re}} R_2\right)\bar{U}_t = -(\bar{U}^n \nabla^h)\bar{U}^n -$$

$$- \operatorname{grad}^h P^n - \frac{1}{\mathrm{Re}} \Delta^h \bar{U}^n - \frac{1}{\beta} \nabla^h A^{-1} \operatorname{div}^h \bar{U}^n,$$

$$\beta\tau (E + \omega A_1)(E + \omega A_2) P_t = \operatorname{div}^h \bar{U}^{n+1}.$$

Each of the brackets in the left-hand sides of the equations is a triangular matrix. Therefore one iteration of the alternately triangular method would suffice to solve the equations obtained. Regularization schemes do not require the statement of conditions for pressure on the boundary of the region and, furthermore, are extremely fast in terms of amount of arithmetic operations on each step. This makes them very effective for calculating nonstationary problems. To prescribe the initial pressure field, the first time step can be made using the scheme of splitting.

We point out that only the application of the very effective method of regularization, LDU-expansion, and the ICCG + ILU method in splitting schemes enabled the authors to efficiently perform modeling of flows in a burner of intricate shape both in the two-dimensional and three-dimensional statement of the problem. Use was made of computational grids of size 100×30 in the two-dimensional (axisymmetric) statement of the problem and $70 \times 25 \times 25$ in the three-dimensional one. The two-dimensional statement of the problem was used for the initial study of the variants of design, and the three-dimensional one was used for a final check of the chosen design. (We note that by virtue of the burner axisymmetry the results of two-dimensional and three-dimensional modeling practically coincide.)

Modeling of a plasma flame at the center of the burner (Fig. 1) presents a substantial problem. The authors made use of a model of flow in which on the basis of a considerable decrease in the gas density inside the plasma the latter is considered impermeable and is modeled as a solid in the gas flow with the condition of slippage of velocity on the flame boundary. Within the framework of the given problem another simplification was also made, i.e., the plasma was considered isothermal. The shape and size of the solid simulating the flame were selected from the results of plasma flame diagnostics [5]. Modeling the plasma flame in greater detail would be an unnecessary complication of the stated problem since a refinement of the gas flow pattern in the flame would not qualitatively affect vortex formation in the space between the flame and the nozzles. However, it is precisely to plasma that the

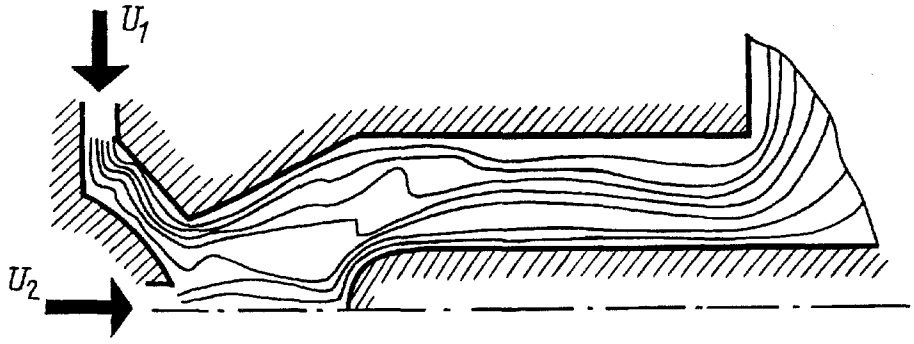

Fig. 4. Vortex-free flow of gases in a burner of optimized shape.

very existence of the problem in question is related: in nonplasma burners there is no need to twist the flow to stabilize the plasma and the recirculation processes considered do not occur there.

In the first stage of modeling, the characteristic vortex structures observed in the plasma burner of the simplest design (Fig. 2) were reproduced. Calculations were performed for burners 10 mm in diameter and 50 mm long and gas flow rates characteristic of the technological process: 5-10 liter/min through the annular nozzle, 0.5-2 liter/min through the central nozzle. As a result of the calculations we found the zone of vortex-free flow in such a burner (Fig. 3); however, it is located in the region of small flow velocities, not ensuring stability of the plasma flame. Figure 3 also shows the results of visual observation of the vortices in a burner of the same geometry using smoke jets.

In subsequent stages of modeling we had to go to gradual complication of the burner geometry, preserving the initial dimensions and gas flow rates. Altogether 16 intermediate variants were considered.

As a result we have obtained the shape of a burner in which the interaction of the gas flows from the basic and annular nozzles leads to practically vortex-free flow in the entire considered range of gas flow rates (Fig. 4). It is shown that with preserved initial dimensions of the burner, recirculation vortices are actively inhibited in the case where the diameter of the narrow section of the burner lies within 3-5 mm and the length of the narrowed portion of the burner is no less than 20 mm.

A plasma burner of such a design is produced at the Institute of General Physics of the Russian Academy of Sciences and has demonstrated high efficiency and prolonged stable operation.

REFERENCES

1. Th. Hunlich, H. Bauch, and R. Th. Kersten, J. Opt. Commun., 8, No. 4, 122-129 (1987).
2. Yu. P. Raizer, Physics of a Gaseous Discharge [in Russian], Moscow (1987).
3. J. Mostaghimi, P. Proulx, and M. J. Boulos, J. Appl. Phys., **61**, No. 5, 1753-1760 (1987).
4. A. S. Biryukov, K. M. Golant, E. M. Dianov, et al., Pis'ma Zh. Tekh. Fiz., 17, No. 5, 80-84 (1991).
5. S. A. Vasiliev, K. M. Golant, E. M. Dianov, et al., Experimental Apparatus for the Emission Spectroscopy of a Superhigh-Frequency Discharge of Atmospheric Pressure [in Russian], Preprint of IOFAN, No. 34, Moscow (1991).
6. J. F. Thompson and Z. U. A. Warsi, Numerical Grid Generation, Foundation and Application, Amsterdam, North Holland (1985), p. 551.
7. A. I. Tolstykh, Zh. Vych. Mat. Mat. Fiz., **21**, No. 2, 339-354 (1981).
8. O. M. Belotserkovskii, Numerical Modeling in Continuum Mechanics [in Russian], Moscow (1984).
9. A. George and J. Lew, Numerical Solution of Large Sparse Systems of Equations [Russian translation], Moscow (1984), p. 333.
10. D. S. Kercaw, J. Comput. Phys., **26**, No. 1, 43-65 (1978).
11. G. M. Kobel'kov, Vestnik MGU, No. 1, 15-22 (1980).